OPTICAL REVIEW Vol. 15, No. 4 (2008) 204–209

Low Tropospheric Wind Measurement with Mie Doppler Lidar

Fahua SHEN, Hyunki CHA[1], Dongsong SUN, Dukhyeon KIM[2], and Sung Ok KWON[1]

Anhui Institute of Optics and Fine Mechanics, the Chinese Academy of Sciences, Hefei 230031, P.R. China
[1]*Korea Atomic Energy Research Institute, Daejeon 305-353, Korea*
[2]*Hanbat National University, Daejeon 305-719, Korea*

(Received January 16, 2008; Accepted April 23, 2008)

A double edge Mie Doppler lidar at 1064 nm was developed in Hefei, China in 2005 for low tropospheric wind measurement. Intercomparison experiments with a wind profiler and a wiresonde were held. Intercomparisons of concurrent lidar and other instrument observations show good agreement with expected measurement accuracy. The examples of validated lidar wind profiles obtained during these experiments as well as an example of continuous wind observations are presented. The instrument has demonstrated the capability of atmospheric wind field measurement from 0.2 to 5 km altitude, achieving below 2 m/s accuracy with 1 min averaging and 21.2 m vertical resolution.

Key words: Doppler lidar, tropospheric wind, Fabry–Perot etalon, Mie scattering

1. Introduction

Instruments for measuring winds in the lower troposphere are indispensable in the study of atmospheric transport of aerosols and other dynamic processes, improving current meteorological modeling and forecasting, identifying possible hazardous weather conditions for aviation such as wind shear from wake vortices and microbursts.[1)] Doppler wind lidar (DWL) has demonstrated its capability to provide vertical wind profiles of the desired accuracy, resolution, and distribution throughout the atmosphere from ground-based and airborne platforms.[2)] It exists in two general categories: heterodyne (or coherent) detection and direct detection (or incoherent) systems. In heterodyne detection, the backscatter signal is mixed with a local oscillator to generate a beat frequency proportional to Doppler shift. For direct detection instruments, the return and the reference signals are independently analyzed using a high resolution frequency discriminator, consequently the Doppler shift can be deduced by comparing the responses and the line-of-sight (LOS) wind velocity can be retrieved. Two direct detection methods are usually employed for the DWL system: fringe-imaging technique[2,3)] and edge technique.[4–9)] The former employs a spectral resolving analyzer to resolve the spectral signature, transforming the Doppler shift to the shift of the interference fringe, which is then projected on a spatially resolving detector and fitted to determine the geometrical displacement of the energetic centroid. The latter uses a high-resolution optical filter, commonly a Fabry–Perot interferometer (FPI), to convert the Doppler frequency shift to an amplitude change.

A direct-detection Mie DWL system at 1064 nm using a double-edge (DE) technique was built at the Anhui Institute of Optics and Fine Mechanics, CAS, Heifei, China and deployed in 2005 for wind measurement.[8,9)] The system is designed to measure the wind profile of the low troposphere, and aimed at verification of the ability of measuring the wind field by aerosol backscattering. The DE method uses two identical high spectral resolution optical filters located symmetrically about the outgoing laser frequency. Using the DE method, the Doppler-shifted aerosol signals can effectively remove the contamination of the molecular backscattering signal to greatly improve the signal to noise in the aerosol rich region.[4)] The details of the DE method have been reported for lidar systems measuring the Doppler shift from either aerosol or molecular backscattered signals.[4,5)]

The instrument has participated in two intercomparison experiments since Sept. 2005. Nearly 100 h of wind measurement under a wide variety of conditions including day and night operation has been obtained: more than 70 h from the Airda16000 wind profiler radar (WPR)-lidar intercomparison experiment during July 15–30, 2006 and about 28 h from the Vaisala wiresonde-lidar intercomparison experiment during September 13–18, 2006, respectively.

This paper will firstly provide a brief review of the instrument and then present the wind measurement results obtained from the aforementioned experiments to validate the instrument, and evaluate its wind measurement accuracy. Then, an additional example of 48 h continuous wind field observations as well as lidar return intensities and wind errors is presented to fully display the stability and robustness of this lidar system.

2. Lidar System Description

Doppler lidar systems generally consist of four major subsystems, which are the laser transmitter subsystem, the telescope subsystem, a detection/receiver subsystem and the controlling subsystem, as shown in Fig. 1. The details of our lidar system design have been described elsewhere[8,9)] and here will be just briefly summarized. A 1064 nm injection-seeded Nd:YAG laser (Continuum, Model 8050) is mounted on an optical bench along with beam pointing optics and a 30 cm aperture telescope. A matching 30 cm aperture scanner which provides full hemispherical pointing using a motor driven azimuth and elevation mirrors is mounted on the roof right above the telescope. The outgoing laser is split in two beams by a beam splitter. Most (99%) of the light is directed through an 8X expander to compress the beam

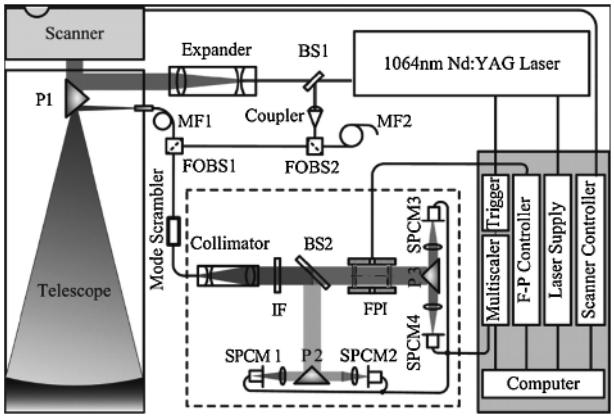

Fig. 1. Schematic of the lidar system: BS, beam splitter; P, prism; MF, multimode fiber; FOBS, fiber-optic beam splitter; IF, interference filter; SPCM, single photon counting mode; FPI, Fabry–Perot interferemeter.

Table 1. Parameters of the aerosol Doppler lidar system.

Item	Parameter
System	
Zenith angle (deg)	45
Wavelength (nm)	1064
Laser energy (mJ/pulse)	100
Laser beam divergence (mrad)	0.5
Optical efficiency (%)	80
Receiver	
Telescope diameter (mm)	ϕ300
Detector type	Si:APD
Quantum efficiency (%)	18
Etalon FSR (GHz)	3.5
Etalon FWHM (MHz)	190
Etalon center interval (MHz)	200
Etalon peak transmittance (%)	>60

divergence, reflected by a mirror mounted in the telescope and points to the atmosphere through the scanner. A small portion (1%) of the outgoing laser is coupled directly into the receiver through an optical fiber as the reference signal. The collected backscatter signal from the telescope is coupled to a 100 μm multimode fiber which transfers the signal into the receiver system. A mode scrambler is mounted on the transfer fiber to unify the illumination intensity on the etalon. The receiver system is shown in the dashed box in Fig. 1. The light from the transfer fiber, collimated by a collimator, passes through an interference filter with the bandwidth of 0.5 nm at 1064 nm and then is split by a beam splitter (80/20) and two prisms into a total of four channels, all of which have Si:APD (avalanche photo diode, Perkin Elmer) detectors operated in single-photon counting mode. Two of them (the "edge" channels) are directed along parallel paths through a dual Fabry–Perot etalon for the detection of Doppler shift. The etalon, capacitively stabilized and piezoelectrically tuned, consists of two semicircular channels with slightly different cavity spacing. This difference of two cavity spacing has been measured to be about 32.5 nm, which corresponds to the central interval of about 200 MHz. The other two channels serve as energy monitor channels which provide intensity normalization of the respective etalon signals during calibration. The radial wind velocity can be uniquely determined by measuring the ratio of the two normalized edge signals. To construct horizontal wind speed and direction, lidar is operated in a step stare scanning mode, in which the lidar stares for some time in three directions, every 120° azimuth sequentially with a 45° zenith angle. The operating commands of laser shooting, XY scanner and Fabry–Perot etalon are sent out by the computer through RS232 interface. Software has been developed to achieve real time signal processing and unattended operation. The key system parameters are listed in Table 1.

The stability of outgoing laser frequency and that of the two etalons are of great importance to the accuracy of the

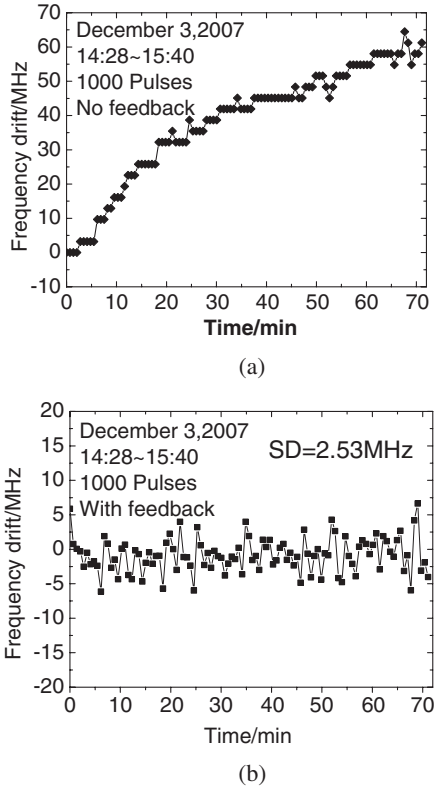

Fig. 2. The long term change of pulse laser frequency. (a) No feedback. (b) With feedback.

velocity measurements. In order to guarantee the wind accuracy, the laser frequency drift or jitter is detected by measuring the real-time reference signal through the Doppler receiver to remove the short-term (less than 20 ms) frequency error effect, and a servo loop is used to lock the etalon to the laser frequency so that the crossover point of the edge filters is always aligned to the laser frequency to eliminate the long-term (on the order of several minutes to several hours) frequency error. Figure 2 shows the long-term change of pulse laser frequency (a) without and (b) with the frequency locking system. By using the servo loop locking

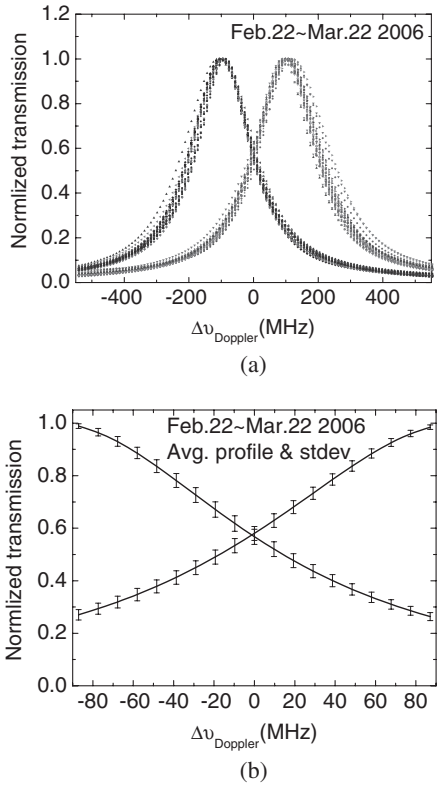

Fig. 3. (a) Measured transmittances for the dual etalon with pulsed laser. (b) Average and standard deviations of transmittances for one month.

system, the frequency variation is drastically reduced to 2.5 MHz (rms). Figure 3(a) shows transmittance curves of the dual etalon measured several times during 1 month. The curves were measured by changing the etalon piezo-voltage while fixing the pulsed laser frequency. The corresponding average transmission is shown in Fig. 3(b). The standard deviations of transmissions were determined to be 1–2.8%, which is mainly caused by the incident angle of the laser beam to the etalon and the efficiency of coupling to each detector which changes due to mechanical quiver. Then, the radial wind measurement error without curve calibration is 0.5–1.3 m/s. In practice, the transmittance curves of the dual etalon are calibrated in advance for each time wind measurement, so the effect of this magnitude long-term drift on wind measurement accuracy is almost eliminated.

3. Lidar Observations

3.1 Intercomparison experiments

3.1.1 WPR-DWL intercomparison

The first one was made between the DWL and a WPR (Airda16000) which was located about 450 m away from the lidar during July 15–30, 2006. The principal goal was to compare horizontal wind profiles from the WPR and the DWL operated nearly coincidentally in space and time under a variety of atmospheric conditions. The wind speed and direction accuracies of WPR are expected to be better than 1 m/s and 10° respectively, with about 150 m spatial resolution and 30 min integration. During the experiment,

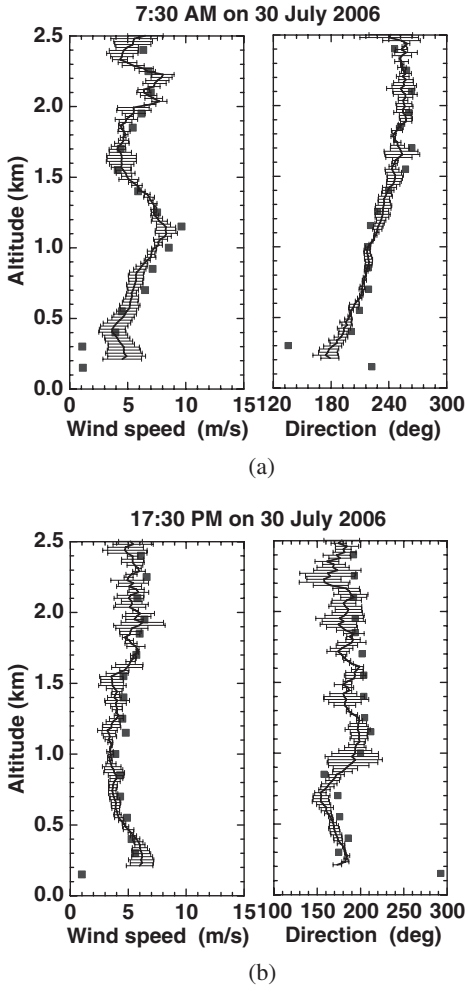

Fig. 4. Horizontal wind speed and direction profiles measured by Doppler wind lidar (solid curve) and wind profiler radar (squares). (a) 7:30 AM on July 30, 2006. (b) 17:30 PM on July 30, 2006.

DWL stared for 1 min in three directions, every 120° azimuth sequentially with a 45° zenith angle. The three direction radial wind profiles were combined to derive the horizontal wind speed and direction every 10 min with a vertical resolution of 21.2 m.

Figures 4(a) and 4(b) are two examples of lidar profiles of wind speed and direction obtained on July 30, 2006 at 7:30am and 17:30pm, respectively. The WPR wind profiles (squares) are also shown for comparison. In these examples, the mean and standard deviation of three consecutive 10 min lidar wind profiles are shown as a function of altitude. The standard deviations, representing a statistical estimate of the random error averaged over altitude, are 0.76 m/s and 6.2° with maximum values of 2 m/s and 30.3°, respectively, from 7:00am to 7:30am, and are 0.69 m/s and 11.8° with maximum values of 2.3 m/s and 32.3° from 17:00pm to 17:30pm. These errors include both instrumental effects and atmospheric variability during the 30 min measurement period. Since the meteorological conditions were mostly stable during the experiment, these data sets were useful for examining the instrumental errors.

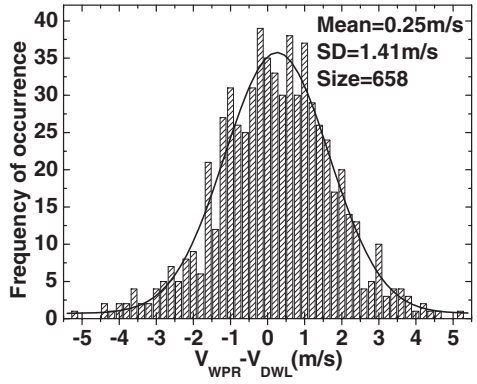

(a)

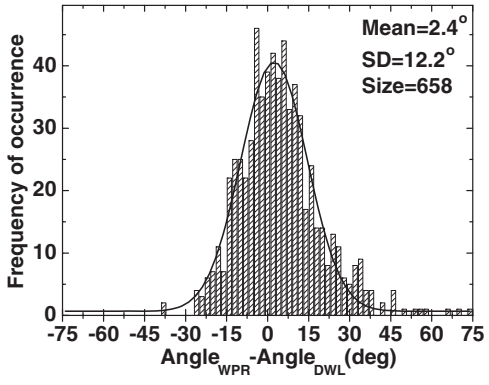

(b)

Fig. 5. Histogram of differences between corresponding pairs of wind speeds (a) and wind directions (b) for the DWL and WPR in common spatial and temporal resolutions.

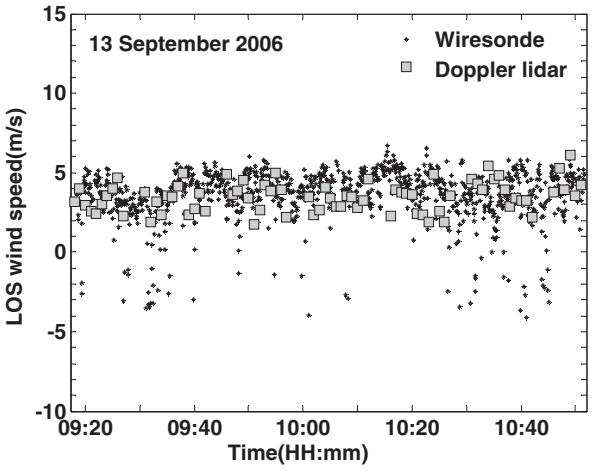

(a)

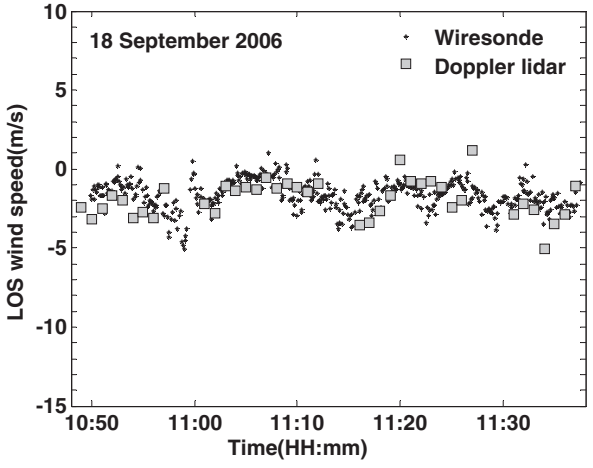

(b)

Fig. 6. LOS wind measured with DWL and wiresonde. The wind lidar measurements are shown as squares and the wiresonde data are shown as asterisks. (a) September 13, 2006. (b) September 18, 2006.

The horizontal wind speed and direction (the angle of the wind direction is clockwise from the north) data from the DWL and WPR show good agreement above about 300 m in Fig. 4. The deviation in the altitude lower than 300 m may be due to the WPR system being affected by the echoes from its surroundings.

Furthermore, for further comparison to the WPR wind data, the DWL data are re-gridded in accordance with the spatial and temporal resolutions of WPR wind data. The cumulative distribution of differences between all collocated (in height and time) wind data pairs from DWL and WPR for an altitude range of 0.55 to 2.4 km on the entire day of July 30, 2006 is shown in Fig. 5, from which one can see that the shape distribution of differences for wind speed and wind direction are both approximately Gaussian. The distribution of differences for wind speed reflects the increased random wind measurement uncertainty of DWL and WPR as reduced backscattered signals are detected from successively greater altitudes. The standard deviations of data pair differences are 1.41 m/s for wind speed and 12.2° for wind direction, respectively, which are contributed from random measurement errors inherent in both DWL and WPR data sets. The mean differences for wind speed and direction are 0.25 m/s and 2.4°, respectively, which indicate the possibility of a small bias between the DWL and WPR data.

3.1.2 Vaisala Wiresonde-DWL intercomparison

Radiosonde is widely regarded as a standard against which other wind observations can be judged. So we conducted another comparison experiment between lidar and Vaisala wiresonde from September 13–18, 2006 to evaluate the accuracy of DWL quantitatively. The wind speed and direction errors of the wiresonde are expected to be 0.5 m/s and 10°, respectively. In the experiment, the laser beam pointed to the direction of the wiresonde horizontally. The temporal resolution of DWL was set to be 1 min, while there were several pieces of measurement data from the wiresonde during this interval. So the wiresonde measured wind data were averaged every minute and then projected to the lidar line of sight for intercomparison. The lidar system was built on the roof of the main building at an altitude of 36.6 m and the wiresonde was hung on the pilot balloon at an altitude of 40 m, just beyond the laser beam. The photon counting signals were binned in a multichannel scalar. Because the horizontal distance between the lidar and the wiresonde is

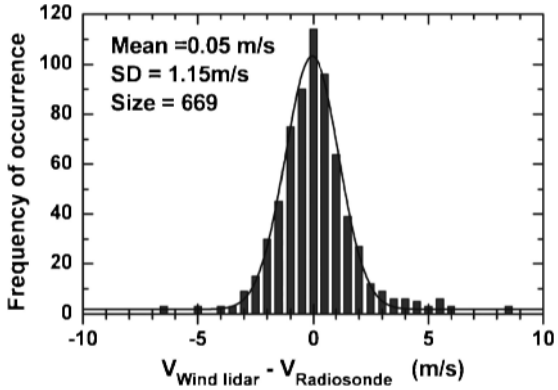

Fig. 7. Histogram of differences between corresponding pairs of 1-min LOS projected horizontal wind velocities for the DWL and wiresonde.

about 480 m and the spatial resolution of DWL was 30 m, we just use the lidar wind data of the 16th bin for comparison.

The lidar measurement results on September 13 and 18, 2006 are shown in Fig. 6. Also shown are wind data determined from wiresonde launched at the corresponding lidar measurement time. The spike points in the wiresonde data may be owing to its wobble in the wind. The stronger the wind, the more spikes were observed. These invalid data were not used for comparsion. The cumulative distribution of differences between the DWL and wiresonde LOS winds for the 5 days is presented in Fig. 7. The distribution is close to normal, as indicated by the goodness of fit of the Gaussian curve plotted over the histogram. The mean difference is 0.05 m/s for large data set, very close to zero. This bias may be due to uncertainties in the system parameters and spectral calibrations during these 5 days. The differences are narrowly and normally distributed with a standard deviation of 1.15 m/s. To assess the "ground truth" accuracy of DWL wind measurement, we consider a standard deviation of 1 m/s was contributed from the wiresonde, in which 0.5 m/s is from the inherent wind speed measurement error and others are from wind direction measurement error of 10° and its wobble. So, the radial wind error of DWL δV_r is 0.57 m/s. Then, for the three beam scanning mode described in §3.1.1, the horizontal wind error $\delta V_h = 2/3^{1/2} \times \delta V_r$ is 0.66 m/s, which is in a good agreement with the standard deviation in Fig. 4.

3.2 *Routine observations*

Continuous operation of the lidar can produce a time series of wind profile data to capture dynamics in the

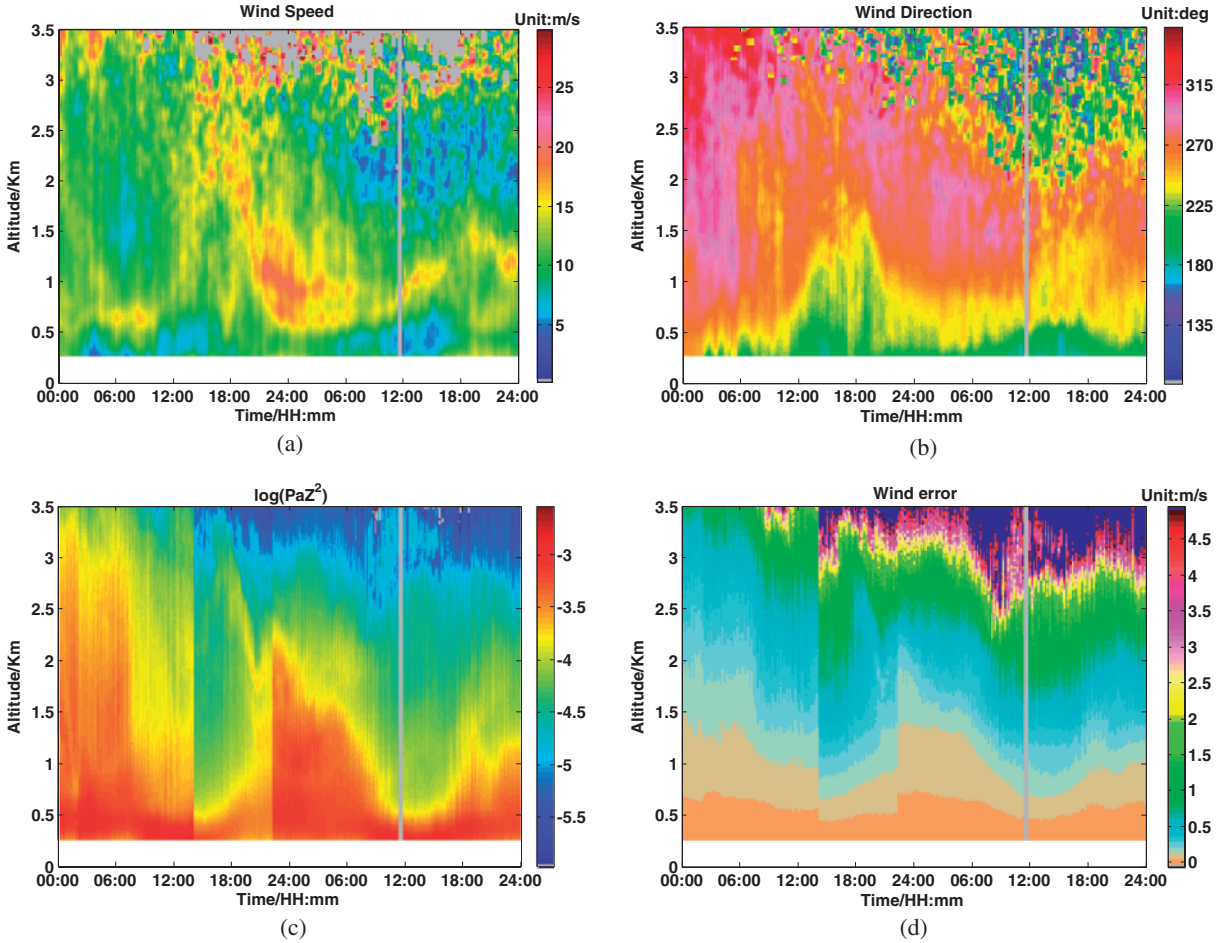

Fig. 8. Time series of lidar wind speed, wind direction, lidar return intensity and wind error profiles obtained on April 29–30, 2006. (a) Wind speed. (b) Wind direction. (c) Range corrected Mie scattering power. (d) Wind velocity error.

boundary layer. Figure 8 shows an example of 48 h of the horizontal wind speed, direction, and range corrected Mie scattering power P_aZ^2 (P_a is the lidar received Mie scattering power, Z is the vertical range) measured by lidar from April 29 to 30, 2006. The three direction radial wind profiles were combined to derive horizontal wind speed and direction. The vertical and temporal resolutions for each horizontal wind profile were 21.2 m and 10 min, respectively. For the initial 12 h, wind profiles could extend for 5 km where the aerosol concentration was still high. The low level jet was observed between 20:40pm of April 29 to 03:00am of April 30. The maximum speed of 20.2 m/s was detected at an altitude of 1.08 km at 21:40pm of April 29. Of particular interest is the pronounced wind speed rise and wind direction change observed from 0.5 to 1.5 km altitude at 20:40pm of April 29. From 20:00pm of April 29 to 20:00pm of April 30, the wind speed and direction below 0.5 km were coincident with the weather forecasting on April 29 which said the wind speed was 4–5 grade (5.5–10.7 m/s) and wind direction was southwest (225°).

The corresponding wind errors are evaluated and shown in Fig. 8(d), from which one can see that below 2.5 km, the range-dependent horizontal wind speed errors were below 2 m/s. The errors increased at the high altitudes due to the gradual decrease in signal return, which can be indicated from the time-height plot of P_aZ^2 in logarithmic scale in Fig. 8(c). For the initial 6 h of nighttime, the wind speed errors were below 1.1 m/s at 3.5 km and wind measurement accuracies better than 2 m/s were obtained up to 5 km in regions of high signal return. From Figs. 8(c) and 8(d), we can see that the wind measurement error will be below 2 m/s if the logarithmic range corrected Mie scattering power $\log(P_aZ^2)$ is larger than -4.5.

A dramatic change of P_aZ^2 values between 14:20pm to 22:30pm on April 29, 2006 was caused by inserting a diaphragm in the transmission path to avoid saturation of the detectors during this time. At the same time, the detectors were gated off below approximately 210 m altitude to avoid saturation. From the time-height plot of $\log(P_aZ^2)$, an abnormal phenomenon of periodical change can be seen. There may be two reasons for this. From Fig. 8(a), strong winds appeared at night blowing up dust near the ground during this season in the region of Hefei. Another reason could be that some useful signals were submerged in the solar background noises in the daytime, and a portion of aerosol backscattering signals was deducted just as noise in the data process. Usually, the measurement errors of wind in the daytime are larger than at night even for the same backscattered signals, and DWL wind detection can extend to higher altitude at night, which is indicated in Fig. 8(d).

4. Conclusions

The horizontal wind profiles measured by DWL were consistent with concurrent WPR observations. Comparisons of pairs of lidar and wiresonde radial wind components showed good agreement and revealed small mean differences, indicating that the DWL system can measure the wind on time scales of as short as one-minute, provided it receives sufficient echoes. Now the system which is housed in a single trailer container is much more stable, compact and more suitable for field operations. This lidar system is able to yield wind measurements routinely with an accuracy of 2 m/s in an aerosol rich environment where the logarithmic range corrected Mie scattering power is larger than -4.5.

Acknowledgements

The authors acknowledge Professors Ningquan Weng and Jun Zhou for their support of the data. They thank Professor Huanlin Hu and Dr. Zhong Zhiqing who gave some instructive advice in the Anhui Institute of Optics and Fine Mechanics.

References

1) J. T. Dobler, B. M. Gentry, and J. A. Reagan: Proc. SPIE **4484** (2002) 354.
2) M. T. Dehring, P. Tchoryk, Jr., and J. Wang: Proc. SPIE **6200** (2006) 6200p-1.
3) W. R. Skinner and P. B. Hays: Proc. SPIE **2266** (1994) 383.
4) C. L. Korb, B. M. Gentry, S. X. Li, and C. Flesia: Appl. Opt. **37** (1998) 3097.
5) C. Flesia and C. L. Korb: Appl. Opt. **38** (1999) 432.
6) B. M. Gentry, H. Chen, and S. X. Li: Opt. Lett. **25** (2000) 1231.
7) M. Imaki and T. Kobayashi: Appl. Opt. **44** (2005) 6023.
8) D. Sun, Z. Zhong, J. Zhou, H. Hu, and T. Kobayashi: Opt. Rev. **12** (2005) 409.
9) H. Xia, D. Sun, Y. Yang, F. Shen, J. Dong, and T. Kobayashi: Appl. Opt. **46** (2007) 7120.